ChemComm

Elucidation of the Resting State of a Rhodium *NNN*-Pincer Hydrogenation Catalyst that Features a Remarkably Upfield Hydride ^{1}H NMR Chemical Shift

Journal:	*ChemComm*
Manuscript ID	CC-COM-10-2015-008348
Article Type:	Communication
Date Submitted by the Author:	07-Oct-2015
Complete List of Authors:	Hänninen, Mikko; University of Lethbridge, Chemistry and Biochemistry Zamora, Matthew; University of Lethbridge, Chemistry and Biochemistry MacNeil, Connor; University of Lethbridge, Chemistry and Biochemistry Knott, Jackson; University of Lethbridge, Chemistry and Biochemistry Hayes, Paul; University of Lethbridge, Chemistry

Chemical Communications ChemComm

Cite this: DOI: 10.1039/c0xx00000x

www.rsc.org/xxxxxx

COMMUNICATION

Elucidation of the Resting State of a Rhodium *NNN*-Pincer Hydrogenation Catalyst that Features a Remarkably Upfield Hydride ^{1}H NMR Chemical Shift

Mikko M. Hänninen,[a] Matthew T. Zamora,[a] Connor S. MacNeil,[a] Jackson P. Knott[a] and Paul G. Hayes*[,a]

Received (in XXX, XXX) Xth XXXXXXXXX 20XX, Accepted Xth XXXXXXXXX 20XX
DOI: 10.1039/b000000x

Rhodium(I) alkene complexes of an *NNN*-pincer ligand catalyze the hydrogenation of alkenes, including ethylene. The terminal or resting state of the catalyst, which exhibits an unprecedentedly upfield Rh–hydride ^{1}H NMR chemical shift, has been isolated and a synthetic cycle for regenerating the catalytically active species has been established.

Although pincer ligands have garnered ever-increasing attention in recent years,[1, 2] the sub-class of monoanionic *NNN*-scaffolds has been less studied than other variants.[3] As a result, our group has focussed on developing a diverse library of these nitrogen-based pincer frameworks for the stabilization of rare earth complexes.[4-6] However, the utility of these species is currently limited to a narrow catalytic scope, and we were interested in expanding our repertoire to include hydrogenation reactivity. As a result, the exceptional utility of platinum group metals in this realm of catalysis[7] and the novel chemistry often induced by hard nitrogen-based ligands bound to soft metals,[3, 8, 9] prompted us to seek new reactivity patterns from late transition metal complexes supported by our *NNN*-pincer ligands. Furthermore, given the propensity for ubiquitous phosphorous-containing pincer ligands to succumb to oxidative degradation,[10] we surmised that nitrogen-capped variants, which are much less prone to such decomposition pathways, could prove particularly useful in stabilizing both robust and unusual late metal complexes.

More specifically, we sought to utilize our recently reported monoanionic, pyrrole-based bisphosphinimine pincer ligands[5] with transition metals that typically form four-coordinate complexes. Pincer systems generally adopt a meridional geometry that can promote access to low-coordinate, 14-electron transition metal species, which participate in various bond activation processes relevant to a plethora of industrially significant catalytic transformations, including hydrogenation.[11, 12] Accordingly, square planar rhodium(I) complexes were identified as appropriate targets for these studies. Notably, although Rh(I) complexes bearing *NNN*-pincer ligands are relatively scarce,[3,13,14-17] those that are known have consistently demonstrated intriguing chemical reactivity. For example, a Rh(I) species bearing a 2,2′:6′,2″-terpyridine ligand was reported to activate O_2 in H_2O upon addition of H_2,[18] a reaction that would have been impossible if traditional phosphine-containing pincers had been utilized. Herein, we report unusual alkene and alkyne Rh(I) hydrogenation catalysts, which exhibit activity comparable to well-known variants, as well as the elucidation of a synthetic cycle that identifies the resting state of the catalyst and permits regeneration of the catalytically active species.

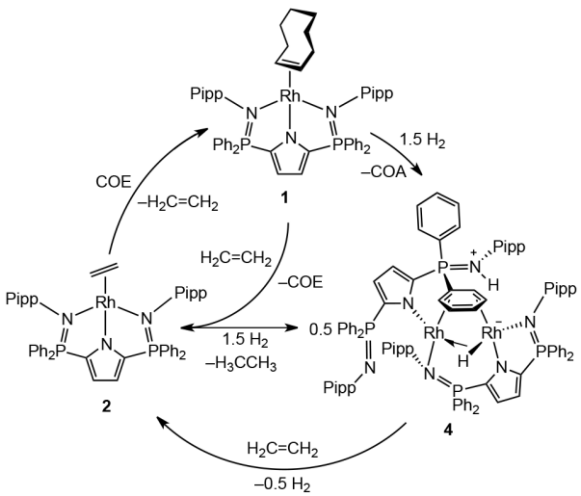

Scheme 1 Synthesis and reactivity of **1**; Pipp = 4-isopropylphenyl, COE = cyclooctene, COA = cyclooctane. Gases were added in excess.

Reaction between the sodium salt (Na**L**•THF[†]) of our bis(phosphinimine)pyrrole ligand **L** and 0.5 equiv of $[RhCl(COE)_2]_2$ (COE = cyclooctene) at 50 °C in toluene cleanly afforded **L**Rh(COE), **1** (**Scheme 1**), after 1 hour, as seen by complete consumption of the $^{31}P\{^1H\}$ NMR resonance for Na**L** (δ 8.8), along with concomitant emergence of a new signal at δ 33.8 that features diagnostic coupling to ^{103}Rh ($^2J_{PRh}$ = 6.0 Hz). In addition, free COE, as well as a dramatic upfield shift and broadening of the resonance attributed to the bound olefin (δ 3.52, $^2J_{HRh}$ = 7.8 Hz, *cf.* δ 5.65 for corresponding protons in non-coordinated COE) were apparent in the ^{1}H NMR spectrum. Finally, the $^{13}C\{^1H\}$ NMR spectrum exhibits properties similar to recently published rare earth complexes ligated by ligand **L**.[5, 19]

Single crystals of complex **1** (**Fig. 1**) were grown from a concentrated toluene solution at –35 °C. As expected, the ancillary ligand **L** coordinates to the metal centre in a tridentate fashion, along with a coordinated COE ligand to form a four-

coordinate structure wherein the geometry at rhodium is best described as distorted square planar. The metrical parameters related to the pincer are in good agreement with previous studies[5, 19] and the Rh–N and Rh–C_{COE} bond lengths are comparable to reported Rh(I)–C_{COE} complexes bearing similar ligands.[20, 21]

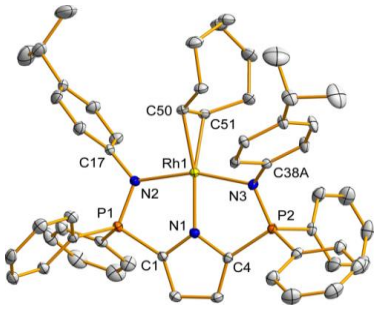

Fig. 1 Molecular structure of complex **1**. Thermal ellipsoids are drawn at the 30% probability level. All hydrogen atoms and minor disordered components have been omitted for clarity. Selected bond distances (Å) and angles (deg): Rh1–N1 = 2.002(2), Rh1–N2 = 2.130(2), Rh1–N3 = 2.145(2), Rh1–C50 = 2.151(2), Rh1–C51 = 2.111(2), C50–C51 = 1.398(4), P1–N2 = 1.608(2), P2–N3 = 1.608(2); C1–P1–N2 = 103.8(1), C4–P2–N3 = 105.4(1), N3–Rh1–N2 = 161.81(8).

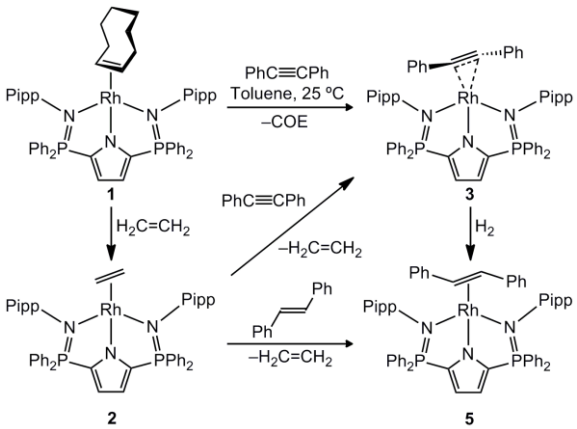

Scheme 2 Reactivity relationships of π-bonded Rh species **1**, **2**, **3** and **5**.

Over the course of 45 min at ambient temperature in benzene-d_6 solution, complex **1** readily reacted with an excess of ethylene to form **L**Rh(H_2C=CH_2), **2** (**Scheme 2**) as evidenced by the disappearance of the coordinated COE signals in the ^{1}H NMR spectrum, along with the materialization of resonances corresponding to a rhodium-coordinated C_2H_4 group (δ 3.14, *cf.* δ 5.22 for free ethylene). In addition, a small but significant frequency change (from δ 33.8 to δ 33.9) was observed for the ^{103}Rh coupled doublet in the ^{31}P{^{1}H} NMR spectrum. X-ray quality crystals of complex **2** were grown from a 2:1:1 benzene:toluene:pentane mixture at –35 ºC; the structure is depicted in **Fig. S1**†. Similarly, complex **1** reacted with a stoichiometric amount of diphenylacetylene to give the anticipated alkyne complex **L**Rh(PhC≡CPh), **3**, and liberated cyclooctene (**Scheme 2**). Diagnostic resonances attributed to coordinated diphenylacetylene were found at δ 8.34, 7.24 and 7.12 in the ^{1}H NMR spectrum of complex **3**. Complex **3** can also be independently prepared by addition of one equiv of diphenylacetylene to the ethylene complex **2**.

Single crystals of complex **3** were grown from a 2:1 benzene:pentane mixture at ambient temperature. As depicted in **Fig. 2**, the distorted square planar coordination sphere about rhodium resembles that observed in **1**. Accordingly, the metrical parameters associated with the ancillary ligand are nearly identical to those in **1** and previously studied complexes.[5, 19] However, the Rh–C bond distances are substantially shorter (Rh–C47 = 2.091(5) Å, Rh–C48 = 2.083(5) Å vs. 2.151(2) Å and 2.111(3) Å) than analogous Rh–C contacts in the alkene complex **1**. Such contraction agrees well with the superior σ-donor and π-donor/acceptor properties of the PhC≡CPh ligand. Although these Rh–C lengths and the slightly bent substituent angles (C48–C47–C55 = 154.4(5)º, C47–C48–C49 = 152.3(5)º) imply partial rehybridization toward sp^2 as a result of π-backbonding from Rh, this moiety befits an η^2 rhodium-bound alkyne description (as opposed to a metallacyclopropene; C47–C48 = 1.229(7) Å).

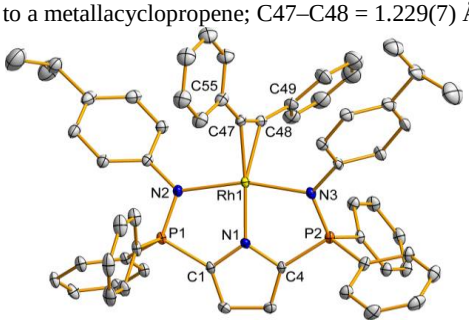

Fig. 2 Molecular structure of complex **3**. Thermal ellipsoids are drawn at the 20% probability level. All hydrogen atoms, solvent molecules of crystallization (benzene) and minor disordered components have been omitted for clarity. Selected bond distances (Å) and angles (deg): Rh1–N1 = 1.976(4), Rh1–N2 = 2.166(4), Rh1–N3 = 2.128(4), Rh1–C47 = 2.091(5), Rh1–C48 = 2.083(5), C47–C48 = 1.229(7), P1–N2 = 1.623(4), P2–N3 = 1.610(4); C1–P1–N2 = 104.1(2), C4–P2–N3 = 103.8(2), N3–Rh1–N2 = 162.91(16), C47–C48–C49 = 154.3(5), C48–C47–C55 = 152.3(6); C55–C47–C48–C49 = 22(2).

The ability of complex **1** to activate H_2 and potentially hydrogenate unsaturated fragments was probed by introducing 1 atm of dihydrogen to an ambient temperature benzene-d_6 solution of the complex. Under these conditions, consumption of H_2 and hydrogenation of COE, as indicated by the appearance of a cyclooctane (COA) signal at δ 1.51 in the ^{1}H NMR spectrum, was observed. Likewise, all COE resonances gradually vanished. Over the course of the reaction, four new signals emerged at δ 31.1 (s), 23.5 (s), 11.8 (d, $^2J_{PRh}$ = 6.2 Hz) and –1.9 (s) in the ^{31}P{^{1}H} NMR spectrum in a 1:1:1:1 ratio. This led us to consider that an asymmetric dinuclear complex, likely the product of self-reaction of a putative 14-electron intermediate, was forming upon ejection of COA from the metal's coordination sphere. Under the same conditions, 1 atm of D_2 yielded **4-*d*$_2$**, along with labelled cyclooctane-d_2 (δ 1.43 in the ^{2}H NMR spectrum) with identical ^{1}H and ^{31}P{^{1}H} spectroscopic signatures for complex **4**.

After 19 h at ambient temperature, complex **1** was completely converted to the aforementioned product. The ^{1}H NMR spectrum, although relatively complicated, exhibits distinct spectral features, including four separate ^{i}Pr methine and eight distinct ^{i}Pr methyl signals, which is consistent with formation of an asymmetric dinuclear complex. Intriguingly, the ^{1}H NMR spectrum comprises an unusually upfield doublet of doublets at δ –35.84 ($^1J_{HRh(1)}$ = $^1J_{HRh(2)}$ = 19.8 Hz), suggesting a remarkably

shielded rhodium hydride ligand. To the best of our knowledge, this signal represents the most upfield chemical shift hitherto reported for any rhodium hydride species.[22, 23] To aid in the complete assignment of **4**, DFT calculations were carried out to predict ^{1}H NMR chemical shifts. In an effort to reduce computational cost, all but the bridging Ph group were replaced with Me groups. Overall, the experimentally-observed chemical shifts are in reasonable agreement with the calculated structure, **4**$^{\prime}$[†]. A deshielded singlet (δ 11.41), attributed to an NH moiety (*vide infra*), is also present. As expected, RhH and NH resonances are absent in the ^{1}H NMR spectrum of **4**-d_2; no evidence of H/D exchange was observed.

The identity of the rhodium-containing product of hydrogenation was unambiguously established by an X-ray diffraction study of high quality crystals grown from a benzene solution layered with pentane at ambient temperature. As can be seen in **Fig. 3**, this zwitterionic species, **4**, is indeed a dinuclear rhodium complex that is the end result of twofold cleavage of H_2 and hydrogenation of COE. This unique product features an interesting RhHRh interaction, as well as an unusual μ-η^2:η^2-bridging phenyl group (**Scheme 1**). Hence, in addition to the shielding effects imparted by two directly-bonded Rh(I) centres, the cause of the abnormally low-frequency hydride ^{1}H NMR chemical shift is presumably a consequence of shielding effects imparted by ring current anisotropy of the bridging phenyl group, which is locked into position directly above the hydride ligand (H1–phenyl centroid = 2.318 Å; average H1–centroid–C(aryl) angle = 90.0°, **Fig. S2**[†]). Although the NH proton is located near the deshielding vicinity of the aryl group, its downfield ^{1}H chemical shift most likely originates largely from the positive charge of the phosphiniminium group; comparable protonated phosphinimine benzofuran ligands and zwitterionic 2-phosphiniminium-arenesulfonates exhibit similar resonances.[24-28]

Complex 4 crystallized as dinuclear neutral units in a monoclinic *C*2/*c* space group. The Rh–H bond lengths are identical, which implies that resonance forms of alternating agostic interactions are likely operative (Scheme S1[†]). However, the coordination sphere about each rhodium centre is slightly different which explains the chemically inequivalent ligand environments apparent in solution-state NMR studies. In addition to the rhodium-hydride (H1) bond, Rh1 is ligated by the pyrrole (N1) and phosphinimine (N2) nitrogens of one bisphosphinimine ligand L_A; the second phosphinimine nitrogen (N3) of L_A is coordinated to Rh2. Since N3 is bound to the adjacent rhodium centre, the remaining coordination site on Rh1 is occupied by the π system of a C=C moiety (C86=C87) from a P–Ph group of a second bisphosphinimine ligand (L_B), which is bound to Rh2 *via* only the pyrrole nitrogen (N4) and another C=C (C82=C83) donor from the aforementioned phenyl substituent. The coordination sphere on Rh2 is completed with an agostic interaction from the adjacent Rh–H bond. The absence of coordination by N5 or N6 is supported by the fact that both atoms are more than 3 Å away from either of the metal centres. Interestingly, as a result of protonation of N6, one of the phosphinimine functionalities was transformed into a phosphiniminium (or aminophosphonium) group. Accordingly, the P–N bond distance (P4–N6 = 1.654(3) Å) has been elongated by almost 0.1 Å compared to the free phosphinimine group (P3–N5 = 1.567(3) Å). Both the hydride and the NH hydrogen were located in the Fourier difference map and refined isotropically.

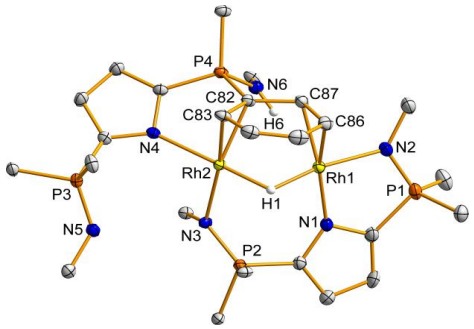

Fig. 3 Molecular structure of **4**. Thermal ellipsoids are drawn at the 30% probability level. All C–H hydrogen atoms, ^{i}Pr groups, solvent molecules of crystallization (benzene), non-*ipso* aryl carbons (except the bridging phenyl group) and minor disordered components are omitted for clarity.

Table 1 Selected bond distances (deg) and angles (Å) of complex **4**.

Rh1–N1	2.060(3)	Rh1···Rh2	2.7689(7)
Rh1–N2	2.120(3)	Rh2–N3	2.118(3)
Rh1–C86	2.170(4)	Rh2–N4	2.103(3)
Rh1–C87	2.091(3)	P1–N2	1.598(3)
Rh2–C82	2.086(3)	P2–N3	1.598(3)
Rh2–C83	2.130(3)	P3–N5	1.567(3)
Rh1–H1	1.70(3)	P4–N6	1.654(3)
Rh2–H1	1.69(3)		
N1–Rh1–C86	158.23(12)	N3–Rh2–C83	165.14(11)
N1–Rh1–C87	163.22(12)	N3–Rh2–C82	155.19(12)
N2–Rh1–Rh2	154.56(9)	N4–Rh2–Rh1	149.51(7)

The bonding in complex **4** can be envisioned several ways, though we believe that a 16e-16e system is most consistent with the diamagnetic NMR spectra obtained in the solution state. Owing to the proximity of both Rh atoms, there is likely some degree of overlap between metal *d*-orbitals; however, addition of a formal metal-metal bond would imply a 17e-17e system, which we believe is misleading. Ultimately, high level computations, which are beyond the scope of this communication, will be necessary to gain a deeper understanding of the bonding interactions within this complex.

Since complex **4** appeared to be the terminal, or resting state of hydrogenation, the reactivity of this complex was of special interest. Significantly, complex **4** could not be converted back to **1** even in the presence of excess COE, or with prolonged heating at 70 °C. Harsher experimental conditions caused decomposition. Likewise, introduction of H_2 in the presence of additional COE did not trigger any reactivity whatsoever. Attempts to generate monomeric species by adding σ-donors (PPh_3, PEt_3, CO) to **4** yielded no change. However, reaction of **1** with one equiv of PPh_3 or an excess of CO afforded L**R**h(PPh_3) and κ^2-*N*,*N*′-L**R**h(CO)$_2$, respectively.[†] Addition of diphenylacetylene to **4** was also investigated as it was thought that the strongly π-donating ligand might afford complex **3**; however, no reaction occurred at ambient temperature and forcing conditions led to the formation of free ligand and multiple intractable by-products. By contrast, when an atmosphere of C_2H_4 was added to a benzene-d_6 solution of **4**, near quantitative conversion to the mononuclear complex **2**

was observed after 96 h at ambient temperature. Intriguingly, ethane formation was also observed, indicating that the bridging hydride and phosphiniminium proton of **4** were either extruded as H_2, or directly transformed **4** into a transient rhodium hydride species that ultimately led to the regeneration of complex **2**. Finally, addition of COE to **2** quantitatively regenerated complex **1** (**Scheme 1**), thus completing the cycle.

Although hydrogenation of C_2H_4 can be challenging,[29] the ethylene complex **2** gratifyingly reacts under 1 atm of H_2 at ambient temperature to produce ethane. Thus, rhodium(I) complexes bearing our *NNN*-pincer **L** are capable of hydrogenating even the smallest alkenes. In addition, the alkyne complex **3** can undergo hydrogenation of its diphenylacetylene ligand to form the *trans*-1,2-diphenylethylene complex **L**Rh(*E*-PhHC=CPhH), **5**, exclusively (**Scheme 2**). An X-ray structure depicting **5** is located in **Fig. S3** of the ESI. Species **5** can also be independently prepared *via* the addition of *trans*-1,2-diphenylethylene to either **1** or **2**. Finally, the catalytic hydrogenation of COE was investigated† with 30–60 equiv of COE consumed under ambient conditions. When compared to Wilkinson's catalyst [chlorotris(triphenylphosphine)Rh(I)], **1** shows an improvement in turnover frequency at >95% conversion (TOF = 12 h^{-1} for Wilkinson's catalyst, 20 h^{-1} for **1**). These exploratory experiments clearly demonstrate the potential of these Rh complexes to serve as diverse hydrogenation catalysts.

In conclusion, this Rh *NNN*-pincer template serves as a gateway to diverse hydrogenation chemistry. In addition to facilitating the catalytic hydrogenation of COE using H_2, the Rh *NNN*-pincer framework in **1** can exchange COE for a variety of other unsaturated hydrocarbons, including ethylene. As a result, the catalyst system tolerates a wide substrate scope, and by virtue of **4** storing both hydridic and protic hydrogen, a synthetic route has been established to renew active Rh–alkene species. In the hydrogenation of diphenylacetylene, the preference to exclusively form the *trans*-stilbene complex **5** suggests that stereoselective processes on more complicated alkynes should be possible, as well as the kinetic resolution of *cis*-variants to preferred *trans*-species. The boundaries of this catalytic potential will be tested in due course, with a focus on regio- and stereoselectivity.

The authors thank the NSERC of Canada for financial support, Prof. Dr. Jun Okuda and RWTH Aachen University for hosting P.G.H. during manuscript preparation, Dr. Tracey Roemmele for combustion measurements, Prof. René Boeré for aid in structure solution of **2**, and Prof. Martin Cowie for helpful discussions.

Notes and references

[a] *Department of Chemistry and Biochemistry, University of Lethbridge, 4401 University Drive, Lethbridge, AB, Canada, T1K 3M4; Fax: 1 403 329 2057; Tel: 1 403 329 2313; E-mail: p.hayes@uleth.ca*

† Electronic Supplementary Information (ESI) available: Experimental and crystallographic details, molecular structures of **2** and **5**, discussion on the structure of **4**, atomic coordinates, interatomic distances and angles, anisotropic thermal parameters, and hydrogen parameters for **1**–**5**. CCDC 1034250–1034254 for **1**–**5**. For ESI and crystallographic data in CIF or electronic format see DOI: 10.1039/b000000x/

1. G. Van koten and D. Milstein, *Organometallic Pincer Chemistry*, Springer Berlin Heidelberg, 2013.
2. D. Morales-Morales and C. M. Jensen, *The Chemistry of Pincer Compounds*, Elsevier, 1st edn., 2007.
3. S. Wanniarachchi, B. J. Liddle, S. V. Lindeman and J. R. Gardinier, *J. Organomet. Chem.*, 2011, **696**, 3623-3636.
4. K. R. D. Johnson and P. G. Hayes, *Organometallics*, 2009, **28**, 6352-6361.
5. K. R. D. Johnson, M. A. Hannon, J. S. Ritch and P. G. Hayes, *Dalton Trans.*, 2012, **41**, 7873-7875.
6. K. R. D. Johnson, B. L. Kamenz and P. G. Hayes, *Organometallics*, 2014, **33**, 3005-3011.
7. A. P. Evans, *Modern Rhodium-Catalyzed Organic Reactions*, WILEY-VCH Verlag GmbH & Co. KGaA, Weinheim 2005.
8. J. L. McBee, J. Escalada and T. D. Tilley, *J. Am. Chem. Soc.*, 2009, **131**, 12703-12713.
9. M. L. Scheuermann, A. T. Luedtke, S. K. Hanson, U. Fekl, W. Kaminsky and K. I. Goldberg, *Organometallics*, 2013, **32**, 4752-4758.
10. P. G. Edwards, R. Haigh, D. Li and P. D. Newman, *J. Am. Chem. Soc.*, 2006, **128**, 3818-3830.
11. C. Gunanathan and D. Milstein, *Science*, 2013, **341**, 249-260.
12. M. E. Boom and D. Milstein, *Chem. Rev.*, 2003, **103**, 1759-1792.
13. W. I. Dzik, C. Creusen, R. de Gelder, T. P. J. Peters, J. M. M. Smits and B. de Bruin, *Organometallics*, 2010, **29**, 1629-1641.
14. C. Tejel, M. A. Ciriano, M. P. del Río, F. J. van den Bruele, D. G. H. Hetterscheid, N. Tsichlis i Spithas and B. de Bruin, *J. Am. Chem. Soc.*, 2008, **130**, 5844-5845.
15. S. Wanniarachchi, B. J. Liddle, B. Kizer, J. S. Hewage, S. V. Lindeman and J. R. Gardinier, *Inorg. Chem.*, 2012, **51**, 10572-10580.
16. D. G. H. Hetterscheid, M. Klop, R. J. N. A. M. Kicken, J. M. M. Smits, E. J. Reijerse and B. de Bruin, *Chem. – Eur. J.*, 2007, **13**, 3386-3405.
17. W. I. Dzik, L. Fuente Arruga, M. A. Siegler, A. L. Spek, J. N. H. Reek and B. de Bruin, *Organometallics*, 2011, **30**, 1902-1913.
18. D. Inoki, T. Matsumoto, H. Hayashi, K. Takashita, H. Nakai and S. Ogo, *Dalton Trans.*, 2012, **41**, 4328-4334.
19. M. T. Zamora, K. R. D. Johnson, M. M. Hänninen and P. G. Hayes, *Dalton Trans.*, 2014, **43**, 10739-10750.
20. P. H. M. Budzelaar, N. N. P. Moonen, R. de Gelder, J. M. M. Smits and A. W. Gal, *Eur. J. Inorg. Chem.*, 2000, **2000**, 753-769.
21. J. D. Masuda and D. W. Stephan, *Can. J. Chem.*, 2005, **83**, 324-327.
22. S. K. Brayshaw, M. J. Ingleson, J. C. Green, P. R. Raithby, G. Kociok-Köhn, J. S. McIndoe and A. S. Weller, *Angew. Chem., Int. Ed.*, 2005, **44**, 6875-6878.
23. C. Kohrt, S. Hansen, H.-J. Drexler, U. Rosenthal, A. Schulz and D. Heller, *Inorg. Chem.*, 2012, **51**, 7377-7383.
24. C. A. Wheaton, B. J. Ireland and P. G. Hayes, *Organometallics*, 2009, **28**, 1282-1285.
25. C. T. Burns, S. Shang, R. Thapa and M. S. Mashuta, *Tetrahedron Lett.*, 2012, **53**, 4832-4835.
26. C. A. Wheaton and P. G. Hayes, *Dalton Trans.*, 2010, **39**, 3861-3869.
27. H. Sun, J. S. Ritch and P. G. Hayes, *Dalton Trans.*, 2012, **41**, 3701-3713.
28. C. A. Wheaton and P. G. Hayes, *Catal. Sci. Technol.*, 2012, **2**, 125-138.
29. J. A. Osborn, F. H. Jardine, J. F. Young and G. Wilkinson, *J. Chem. Soc. A*, 1966, 1711-1732.